NANO LETTERS

LETTER

pubs.acs.org/NanoLett

Near-Field Dynamics of Optical Yagi-Uda Nanoantennas

Jens Dorfmüller,*[,†] Daniel Dregely,[†] Moritz Esslinger,[‡] Worawut Khunsin,[‡] Ralf Vogelgesang,[‡] Klaus Kern,[‡,§] and Harald Giessen[†]

[†]4. Physikalisches Institut und SCoPE Forschungszentrum, Pfaffenwaldring 57, Universität Stuttgart, 70569 Stuttgart, Germany

[‡]Max-Planck-Institut für Festkörperforschung, Heisenbergstrasse 1, 70569 Stuttgart, Germany

[§]Institut de Physique de la Matière Condensée, École Polytechnique Fédérale de Lausanne, 1015 Lausanne, Switzerland

Supporting Information

ABSTRACT: We present near-field measurements of optical Yagi-Uda nanoantennas that are used in receiving mode. The eigenmode imaging of amplitude and phase by apertureless scanning near-field optical microscopy allows us to investigate the dynamics of the local out-of-plane electric field components and to visualize the temporal evolution of this time-harmonic reception process. The antenna directionality manifests itself by the dependence of the local field enhancement at the feed element on the illumination direction. Simulations taking into account the substrate confirm our observation of the directionality. Our work demonstrates the possibility to characterize multielement nanoantennas by electromagnetic antenna near-field scanners.

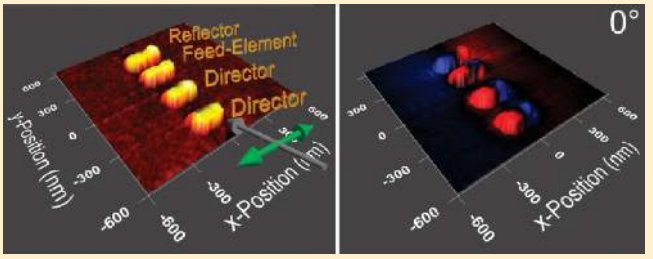

KEYWORDS: Optical nanoantenna, Yagi-Uda antenna, near-field optics, scanning near-field optical microscopy, plasmonics

Over the past few years, increasingly sophisticated structuring techniques enabled the fabrication of metal nanostructures with nearly arbitrary shapes.[1] Simultaneously, certain types of metal nanostructures have gained a firm recognition as optical nanoantennas,[2,3] capable of both enhancing the emission as well as directing the emitted electromagnetic waves.[4,5] Optical antennas may be seen as impedance matching devices between free space radiation and the radiation/photon source. This is especially interesting for the development of more efficient single photon sources as needed in quantum cryptography.[6] Similarly, in receiving mode the antenna is able to confine free space radiation to a subwavelength region in the vicinity of the structure.[7] This could have technological applications in building single photon detectors on the nanoscale. Despite some differences between optical nanoantennas and their radio frequency (RF) counterparts,[8−10] it has been shown that most RF antenna concepts remain applicable in the optical regime.[11−13]

A large and growing body of research investigates directional nanoantennas. Most studies focus on theory and simulation[14,15] and only recently first operational implementations have been demonstrated.[16,17] Antenna directionality in emission mode was nicely proven in these works by far-field spectroscopic imaging of reciprocal space. Our present work aims to fill the complementary gap of experimental near-field investigations. It allows us to draw direct conclusions about the exact antenna mode of operation, which may otherwise only be inferred from simulations mimicking experimental results.

We investigate the optical analogue of the well-known RF Yagi-Uda antenna,[18] namely, the Yagi-Uda nanoantenna, in reception mode with a near-field microscopy technique. Compared to other methods our cross-polarization apertureless scanning near-field optical microscope (aSNOM) allows us to study experimentally the individual antenna elements.[19,20] The ability to simultaneously image amplitude and phase of the normal E-field component around the nanoantenna[21] allows direct investigation of the coupling mechanisms of the particle plasmon resonances to the incident light. We observe the capacitive coupling of the directors and the inductive coupling of the reflector as a phase difference to the feed element. Upon illumination from forward incidence, the retardation of the incident field and the mutual coupling between the elements leads to a constructive interference at the subwavelength sized feed element. This retardation and mutual coupling are also the source of directionality of a resonantly tuned optical Yagi-Uda nanoantenna. For the time harmonic dynamics of the receiving antenna, we use the amplitude and phase information to animate the time evolution of the fields in the reception process.

Materials and Methods. Our experimental scheme is illustrated in Figure 1. The antenna is illuminated from the air side of the substrate by a weakly focused (NA = 0.25) laser beam (wavelength λ = 1064 nm, InnoLight Mephisto) under an oblique angle of 70° (gray arrow) with respect to the surface normal. The horizontal polarization of the light (green arrow) excites localized particle plasmons on the linear antenna elements. To measure the near-fields we use a silicon atomic force microscope tip (Nanosensors, advancedTEC) with a tip radius of

Received: April 8, 2011
Revised: May 19, 2011
Published: May 27, 2011

typically 10 nm as local scatterer. The influence of our silicon tip on the plasmonic resonances is negligible due to the use of crossed light polarizations.[8,20−22] The weak polarizability perpendicular to the tip axis leads to a weak coupling of the tip to the far-field illumination. The near-field components of the excited structure polarized parallel to the tip axis (red and blue arrows) couple to the tip and are scattered back into the far-field where a beam splitter separates the incident from the reflected light.[20,21,23] An analyzer in front of our detector (InGaAs, FEMTO Messtechnik GmbH) selects the light polarized along the tip axis. Careful adjustment of the polarization axes of polarizer and analyzer as well as a tip-sample modulation and higher harmonic demodulation scheme suppresses background signals originating from scattering of the macroscopic tip shaft and the sample. A homodyne optical amplification scheme allows us to detect the optical amplitude as well as the optical phase. In order to image our sample, we raster scan the sample underneath the tip.[19]

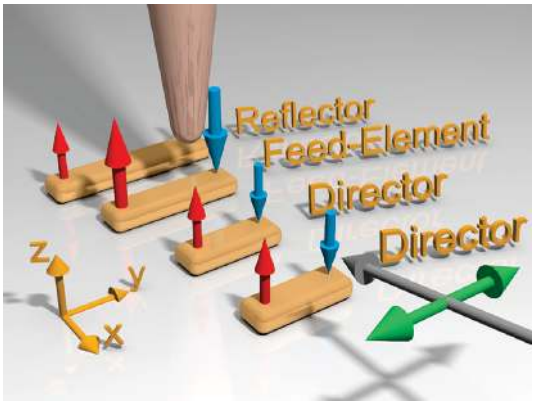

Figure 1. Experimental setup: A Yagi-Uda nanoantenna fabricated on a glass substrate is illuminated by a weakly focused s-polarized (green arrow) laser beam (λ = 1064 nm) under an oblique incident angle (gray arrow). The normal components of the near-fields surrounding the antenna elements (blue and red arrows) can couple to a mode of a sharp AFM tip and are scattered back into the far field.

We fabricate our nanoantennas on a transparent glass substrate by electron beam lithography. This system (Raith, e_LiNE) defines the structures in a spin-coated film of positive resist (PMMA). After evaporation of 3 nm chromium as adhesion layer, we deposit 30 nm gold followed by a lift-off process. The wires forming the antenna elements (Figure 2a) all have a nominal width of 80 nm. The feed element (director, reflector) of the resonant antenna has a nominal length of 198 nm (168, 229 nm, respectively). The distance between feed element and reflector is 210 nm, between the other neighboring antenna components 270 nm.[17] In order to study the size dependence of the resonances, we fabricate a set of antennas 2 μm apart from each other (center to center distance) with different antenna sizes. We varied the nominal length of the feed element (reflector, directors) in 10 nm (12, 9 nm respectively) steps.

The design process of the antenna was facilitated by finite integration technique (FIT) simulations (CST Microwave Studio). The retardation due to the obliquely incident light as well as the interface between air and glass (n = 1.46) was taken into account in the numerical calculations. For the near-field images obtained from these simulations, we used a permittivity of gold described by a Drude model (ω = 1.37 × 10^{16} rad/s, γ = 1.2 × 10^{14} rad/s) fitted to data taken from the literature.[24]

Results and Discussion. Figure 2 shows a three-dimensional view of the topography data from a measurement on a resonant optical Yagi-Uda nanoantenna illuminated under the conditions as illustrated in Figure 1. With the aSNOM being able to measure amplitude and phase, we can reconstruct the field evolution of the time-harmonic reception processes. Panels b−d of Figure 2 show the real part of the E-fields measured above the antenna at different snapshots in time. The electric field strength at the specific incident of time is color coded as texture on top of the 3D

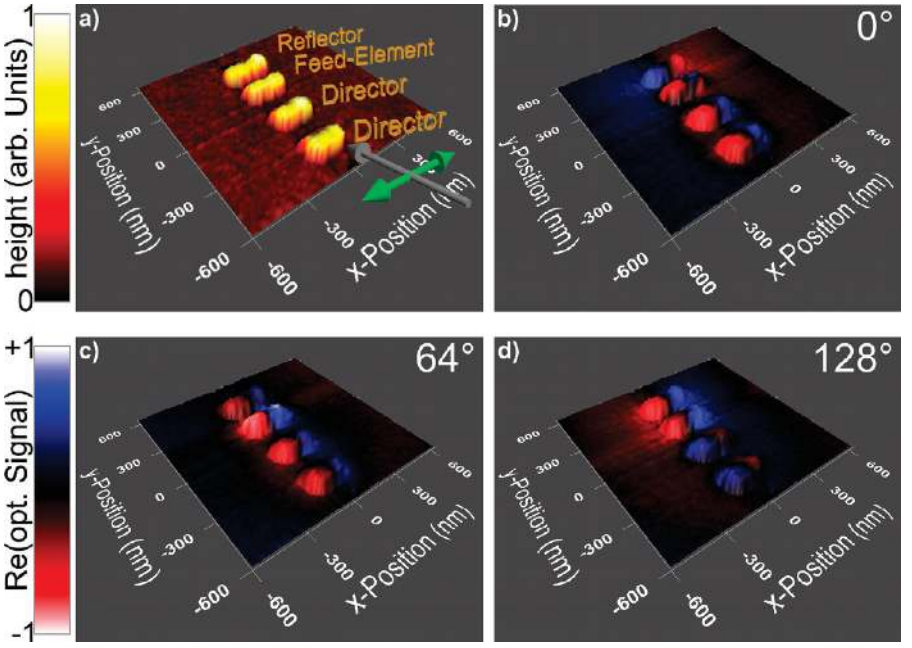

Figure 2. (a) 3D topography of the resonant optical Yagi-Uda antenna. (b−d) Real part of the measured optical signal superimposed onto the topography at different incidents of time: (b) 0° phase, (c) 64° phase, (d) 128° phase. The antenna is illuminated from the front direction, similar to the illumination shown in Figure 1. A full animation can be found as a movie in the Supporting Information.

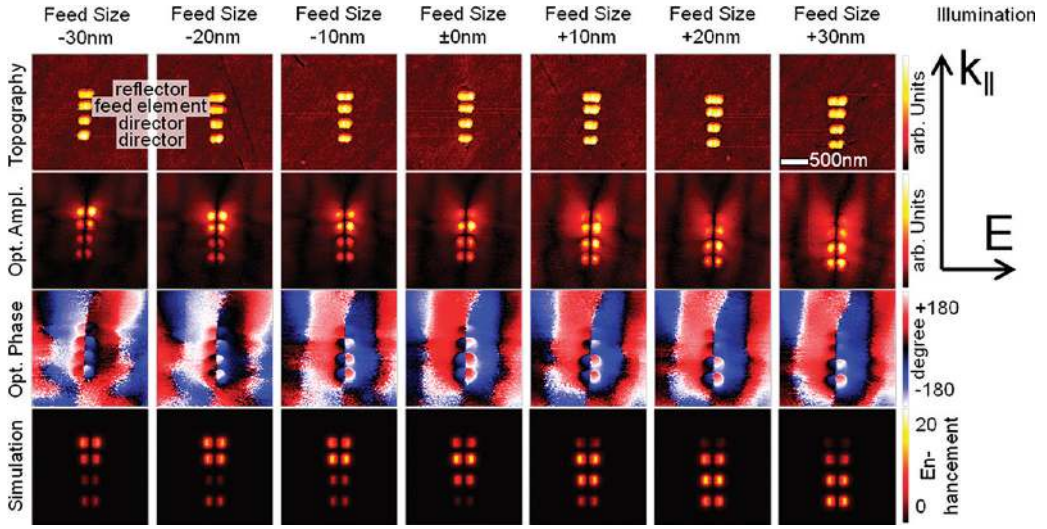

Figure 3. The topography images in the top row show Yagi-Uda nanoantennas of different sizes. This size tuning has a strong influence on the observed near-field images. With increasing antenna size the region of strongest field shifts from the reflector via the feed element to the directors. The simultaneously measured phase images reveal different coupling mechanisms of the antenna elements. The bottom row shows near-field enhancement obtained from simulations for comparison.

topography shown in Figure 2a. Figure 2b shows the fields at the incident of time that we denominate with the phase of 0° where the two directors light up. The two directors show one positive and one negative field lobe with a field node in between them. The feed element shows a rather weak field amplitude, indicating that the fields are close to the point in time where the sign of the field amplitude flips. The reflector shows a dipole pointing in the opposite direction with respect to the directors. Figure 2c shows the situation 64 phase degrees later in time. All antenna elements show the same color scheme, indicating that the dipole moments have the same orientation. The feed element is at its maximum field strength, brighter than all the other elements at any time. Finally, Figure 2d shows the E-fields another 64° later where the reflector reaches its maximum. The field strength of the feed element is already declining and the dipole moments of the upstream lying directors have already flipped. The full animation of the time evolution of the fields around optical Yagi-Uda nanoantennas is included as movie in the Supporting Information.

A high concentration of optical energy at the feed element can only be achieved for an antenna geometry matching the radiation wavelength. In order to study the tuning behavior, we keep the illumination wavelength fixed but tune the size of the antenna (Figure 3). The 10 nm differences in length between feed elements of consecutive antennas are only visible upon careful comparison of the topography images shown in the top row. The optical amplitude, though, shows strong differences. In the very left column, the strongest near-field signal is located at the reflector. With increasing size the strong near-field amplitude is slowly displaced to the feed element. The resonant antenna (labeled ±0 nm) shows a strong localization of the fields at the feed element. Increasing the size even further leads to a diminishing signal at the feed element and the reflector until the maximal signal is located at the directors. This trend is very well reproduced by the simulations shown in the bottom row. The phase images give information how the individual antenna elements are coupled to the surrounding electric fields. With phase stability over at least one whole image, our instrument allows us to measure relative phases. It gives us the possibility to draw conclusions from the phase differences between the antenna elements. In the left column, the directors and the feed element show the same phase pattern and are oscillating in phase. With both of them still being smaller than their resonance size, they are coupled capacitively to the incident field. Compared to these elements, the slightly larger reflector has already picked up some additional phase. For the resonant antenna, the phase difference between directors and reflector reaches nearly 180°, with the feed element having a phase in between the two. While the directors are still capacitively coupled, the reflector is now being inductively coupled to the incident field.

A critical reader might suggest that our observations can be understood in terms of length tuning of the individual linear antenna elements through resonance.[8] To demonstrate that this simple effect is not the source of our observations, we rotate the sample so that we illuminate the antenna from the backward direction (Figure 4). When we tune the size of the feed element through the antenna resonance, we do not observe a phase difference between the feed element and the larger reflector in the phase images. Instead of seeing all antenna elements going through a resonant length in amplitude images, we see how first the reflector lights up (−10 nm), then feed element and reflector together light up (±0 nm), and at last the energy is distributed between all elements (+10 nm). The near-field concentration at the feed-element is missing upon backward illumination. Upon illumination from the front, the retardation of the incident light beam leads to a constructive interference of the scattered light from the directors and the reflector at the feed element, rendering the feed element to appear much brighter than the other elements. With the change of illumination direction this interference turned to a destructive one, suppressing the resonance of the feed element. *The differences between the near-field images for forward and backward illumination of the same structures are clear proof of the antenna directionality.* The forward/backward ratio of the nanoantenna is the key characteristic for its functionality assessment. Measurement of the angular-dependent characteristics is in principle possible with our method[8] but would require a rather time-consuming experimental effort.

dx.doi.org/10.1021/nl201184n |*Nano Lett.* 2011, 11, 2819–2824

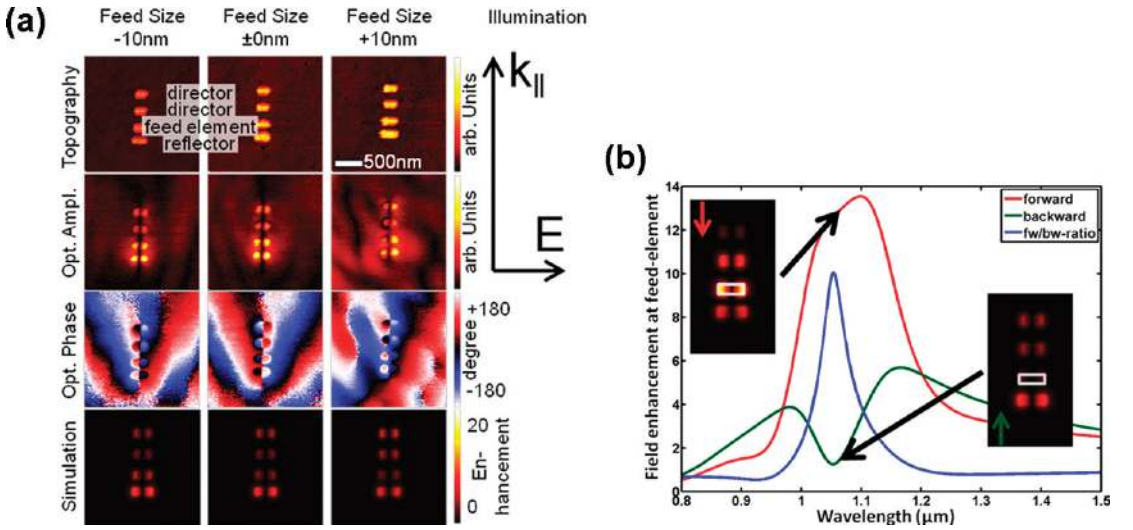

Figure 4. (a) Upon illumination from the backward direction, the tuning of the nanoantenna size shows no clear sign of resonant field enhancement at the feed element. This experimental observation is confirmed by simulations shown in the bottom row. (b) Simulations of the actual antenna geometry allow us to look at the spectral tuning behavior. At the illumination wavelength the antenna shows a peak in the forward/backward-ratio of the *E*-field strength at the feed element.

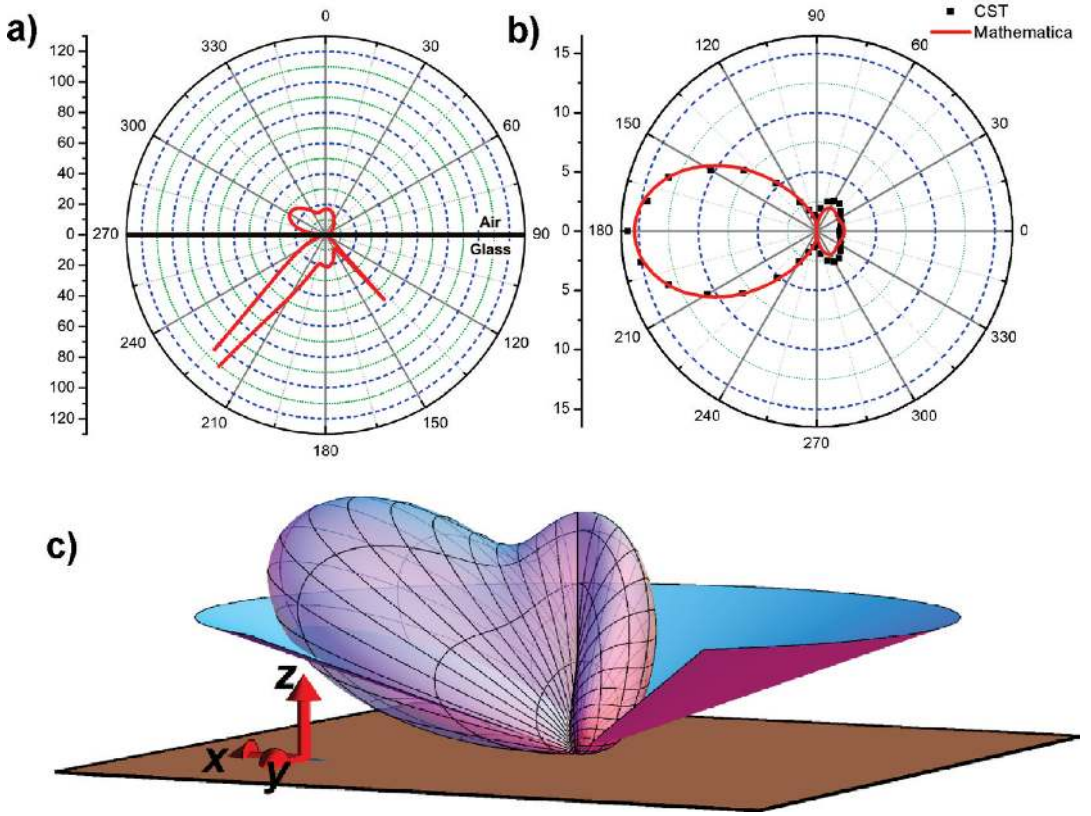

Figure 5. Theoretical predictions of the emission pattern of a substrate supported Yagi-Uda nanoantenna coupled to a dipole emitter. (a) Vertical cut along the $x-z$ plane through the emission pattern. Although most of the electromagnetic radiation is emitted into the critical angle, the above surface emission still shows a strong directivity. (b) Cut through the emission pattern of Yagi-Uda antenna on the air side of the substrate under the angle accessible to our aSNOM: red curve, analytical solution (transmitting mode); black squares, simulation (reception mode). (c) 3D plot of the emission pattern. The cone indicates the illumination angle of our setup.

While in our experimental data we examine the geometrical tuning of the structure, we can use the simulations to investigate the spectral properties of our antennas as well. With the actual geometric parameters of our resonant structure obtained from electron microscopy, we simulate the near-fields of the illuminated antenna and extract the amplitude of the normal *E*-field component

dx.doi.org/10.1021/nl201184n |*Nano Lett.* 2011, 11, 2819–2824

at the feed element. In the spectrum for backward illumination (Figure 4b), we observe a minimum at 1050 nm, while the forward illumination spectrum shows a peak at slightly longer wavelength. The ratio of the forward and the backward spectrum with a peak value of more than 10 shows that the near-field intensity difference is strongest at about our illumination wavelength.

This interpretation of our experimental data is independent of the surrounding media. It is well-known that emitters at the surface between two interfaces emit mainly into the medium which is optically denser in the case that the emission direction is close to the critical angle.[25,26] Recently this was observed in Yagi-Uda nanoantennas on substrates, and interestingly a forward/backward antenna directionality was preserved.[16]

In order to show that our Yagi-Uda antenna on the glass substrate maintains its directionality also in the optically thinner medium, we employ a similar approach as described in the supplementary material of ref 16 and simulate the Yagi-Uda antenna with a dipole emitter coupled to the feed element. From the simulation we extract amplitude and phase of the currents inside the wires and calculate analytically the far-field pattern of four horizontally orientated, interfering dipole emitters which replace our antenna elements.[25] The vertical cut shown in Figure 5a shows the emission into the critical angle as well as a small emission lobe into the air side of the surface. Our oblique incident illumination scheme gives us access to a cone-shaped part of the radiation pattern with an opening angle of approximately 140° as indicated in Figure 5c. The conical cut through the emission pattern shown in Figure 5b shows a strong directionality. Applying the Rayleigh-Carson reciprocity theorem,[27] we expect to observe the same behavior in the reception pattern. Indeed, when we extract the reception characteristic from simulations where we illuminate the antenna by a plane wave under the same oblique angle and take the substrate into account, we observe excellent qualitative agreement between radiation and receiving pattern.

Summary and Outlook. We have shown experimentally that optical Yagi-Uda nanoantennas on a glass substrate show a strong directionality in receiving mode when illuminated from the air side. In the phase channel of our near-field images, we observe the capacitive coupling of the director elements and the inductive coupling of the reflector element. Upon forward illumination of the antenna, the constructive interference of scattered light by these elements leads to a strong field enhancement at the position of the feed element. Upon backward illumination, our measurements reveal that the destructive interference at the position of the feed element suppresses the strong fields. Instead, the optical energy is distributed over the four antenna elements. The interpretation of amplitude and phase dynamics of the Yagi-Uda nanoantenna elements is analogue to their RF counterpart. This suggests that modification of existing RF antenna theories could make it possible to transfer RF engineering design rules also to nanoantennas.[28]

Our observations also show the capability of our aSNOM technique to experimentally examine nanoantennas locally.[21,29,30] While high-resolution techniques that involve electron microscopes, e.g., cathodoluminescence, also reach lateral image resolution well beyond the diffraction limit, they do not offer access to the optical phase.[31] Our simultaneously obtained high-resolution amplitude and phase information give access to the complete antenna dynamics and allow a better insight into the working principle of the individual nanoantenna. With optical nanoantennas being suggested for future interfaces to computer processors[32] or as direct antenna links for connections within a processor,[33,34] the testing of actual structures will gain more importance over the next years. Similar to antenna near-field scanners, a standard tool in RF antenna testing, our apertureless SNOM technique serves as a spatially resolving characterization tool for optical nanoantennas.[35]

■ ASSOCIATED CONTENT

Supporting Information. A movie file showing the experimentally measured local electric field dynamics of the receiving antenna. This material is available free of charge via the Internet at http://pubs.acs.org.

■ AUTHOR INFORMATION

Corresponding Author
*E-mail: J.Dorfmueller@physik.uni-stuttgart.de.

■ ACKNOWLEDGMENT

We acknowledge support by the DFG (SPP1391, FOR557, and FOR730), the BMBF (METAMAT) and the Baden-Württemberg Stiftung (Kompetenznetz Funktionelle Nanostrukturen).

■ REFERENCES

(1) Halas, N. J. *Nano Lett.* **2010**, *10*, 3816–3822.
(2) Mühlschlegel, P.; Eisler, H.-J.; Martin, O. J. F.; Hecht, B.; Pohl, D. W. *Science* **2005**, *308*, 1607–1609.
(3) Bharadwaj, P.; Deutsch, B.; Novotny, L. *Adv. Opt. Photonics* **2009**, *1*, 438–483.
(4) Greffet, J.-J. *Science* **2005**, *308*, 1561–1563.
(5) Taminiau, T. H.; Stefani, F. D.; Segerink, F. B.; van Hulst, N. F. *Nat. Photonics* **2008**, *2*, 234–237.
(6) Lounis, B.; Orrit, M. *Rep. Prog. Phys.* **2005**, *68*, 1129–1179.
(7) Giessen, H.; Lippitz, M. *Science* **2010**, *329*, 910–911.
(8) Dorfmüller, J.; Vogelgesang, R.; Khunsin, W.; Rockstuhl, C.; Etrich, C.; Kern, K. *Nano Lett.* **2010**, *10*, 3596–3603.
(9) Novotny, L. *Phys. Rev. Lett.* **2007**, *98*, 266802.
(10) Taminiau, T. H.; Stefani, F. D.; van Hulst, N. F. *Nano Lett.* **2011**, *11*, 1020–1024.
(11) Esteban, R.; Teperik, T. V.; Greffet, J.-J. *Phys. Rev. Lett.* **2010**, *104*, 1–4.
(12) Li, J.; Salandrino, A.; Engheta, N. *Phys. Rev. B* **2007**, *76*, 245403.
(13) Pakizeh, T.; Käll, M. *Nano Lett.* **2009**, *9*, 2343–2349.
(14) Taminiau, T. H.; Stefani, F. D.; van Hulst, N. F. *Opt. Express* **2008**, *16*, 10858–10866.
(15) Ahmed, A.; Gordon, R. *Nano Lett.* **2011**, *11*, 1800–1803.
(16) Curto, A. G.; Volpe, G.; Taminiau, T. H.; Kreuzer, M. P.; Quidant, R.; van Hulst, N. F. *Science* **2010**, *329*, 930–933.
(17) Kosako, T.; Kadoya, Y.; Hofmann, H. F. *Nat. Photonics* **2010**, *4*, 312–315.
(18) Yagi, H. *Proc. IRE* **1928**, *16*, 715–741.
(19) Bek, A.; Vogelgesang, R.; Kern, K. *Rev. Sci. Instrum.* **2006**, *77*, 043703.
(20) Esteban, R.; Vogelgesang, R.; Dorfmüller, J.; Dmitriev, A.; Rockstuhl, C.; Etrich, C.; Kern, K. *Nano Lett.* **2008**, *8*, 3155–3159.
(21) Dorfmüller, J.; Vogelgesang, R.; Weitz, R. T.; Rockstuhl, C.; Etrich, C.; Pertsch, T.; Lederer, F.; Kern, K. *Nano Lett.* **2009**, *9*, 2372–2377.
(22) Schnell, M.; Garcia-Etxarri, A.; Huber, A. J.; Crozier, K. B.; Borisov, A.; Aizpurua, J.; Hillenbrand, R. *J. Phys. Chem.* **2010**, *114*, 7341–7345.

(23) Zentgraf, T.; Dorfmüller, J.; Rockstuhl, C.; Etrich, C.; Vogelgesang, R.; Kern, K.; Pertsch, T.; Lederer, F.; Giessen, H. *Opt. Lett.* **2008**, *33*, 848–850.
(24) Johnson, P. B.; Christy, R. W. *Phys. Rev. B* **1972**, *6*, 4370–4379.
(25) Novotny, L.; Hecht, B. *Principles of Nano-Optics*; Cambridge University Press: Cambridge, 2006.
(26) Weyl, H. *Ann. Phys. (Weinheim, Ger.)* **1919**, *60*, 481–500.
(27) Carson, J. R. *Bell Syst. Tech. J.* **1924**, *3*, 393–399.
(28) King, R. W. P.; Fikioris, G. J.; Mack, R. B. *Cylindrical Antennas and Arrays*, 2nd ed.; Cambridge University Press: Cambridge, U.K., 2002.
(29) Jones, A. C.; Olmon, R. L.; Skrabalak, S. E.; Wiley, B. J.; Xia, Y. N.; Raschke, M. B. *Nano Lett.* **2009**, *9*, 2553–2558.
(30) Schnell, M.; Garcá-Etxarri, A.; Huber, A. J.; Crozier, K.; Aizpurua, J.; Hillenbrand, R. *Nat. Photonics* **2009**, *3*, 287–291.
(31) Vogelgesang, R.; Dmitriev, A. *Analyst* **2010**, *135*, 1175–1181.
(32) Miller, D. A. B. *Proc. IEEE* **2009**, *97*, 1166–1185.
(33) Alù, A.; Engheta, N. *Phys. Rev. Lett.* **2010**, *104*, 213902.
(34) Dregely, D.; Taubert, R.; Dorfmüller, J.; Vogelgesang, R.; Kern, K.; Giessen, H. *Nat. Commun.* **2011**, *2*, 267.
(35) Yaghjian, A. *IEEE Trans. Antennas Propag.* **1986**, *34*, 30–45.